

# Influence of high-angle grain boundaries on the charge order formation in the $\text{YBa}_2\text{Cu}_3\text{O}_{7-x}$

Vladimir S. Boyko and Roman Ya. Kezerashvili

Physics Department, New York City College of Technology, The City University of New York,  
Brooklyn, NY 11201, USA

We are examining the possibility of the formation of charge order in the high-temperature superconductor  $\text{YBa}_2\text{Cu}_3\text{O}_{7-x}$  (YBCO) due to interaction between the charged oxygen vacancies or di-vacancies. The molecular dynamics method is used to analyze the displacement fields around these defects. The distribution of displacements around a single charged oxygen vacancy and di-vacancy, determination of binding energy of oxygen vacancy in di-vacancy demonstrate that there is, in principle, the possibility of the charge order formation in YBCO by charged oxygen vacancies or di-vacancies. It is shown that the charge order formation first of all should be formed near crystal lattice defects and that the high-angle grain boundaries (GBs) regions are preferable places for this formation. The adsorption capability of high-angle GBs with respect to the stripe embryo formation is determined. It is shown that there is a proportional dependence between the repetition distance along the high-angle GBs and an energy advantage of the stripe embryo formation in GBs.

PACS numbers: 42.70.Qs, 74.25.Gz, 85.25.-j, 78.67.-n

## I. INTRODUCTION

There are many circumstances in which the charge order plays a significant role in the physics of electronically interesting materials [1]. The 1D charge order intensively discussed now in the physics of high-temperature superconductivity (see, for example, [1, 2, 3]). In this case, a spin and charge separate into different linear regions or stripes [4, 5, 6]. It was discovered in [7] that small changes in the crystal structure of high- $T_c$  superconductors can cause disappearance of superconductivity with a static stripe phase taking over. According to Ref. [3], the existence of static stripes, initially contentious, is now generally accepted. However, the structure of charge stripes and conditions of their formation are not well understood.

The consideration [8, 9] showed, that the sheet or stripe phases appears quite naturally if the dominant interaction is the elastic interaction between impurities which is a long-range and intrinsically anisotropic (attractive in certain directions and repulsive in others). It is reasonable to suggest that, in the case of the high- $T_c$  superconductors, more perspective is the consideration of a long-range elastic interaction between oxygen vacancies as the factor stabilizing charge order. Usually, the oxygen vacancies are much more abundant in the high-temperature superconductors than in impurities because of the stoichiometry reasons. To perform the scheme considered in Ref. [8] we need to know the "strength" of the point defect – a local change of the lattice volume at the vacancy location. Then, following the method developed in Ref. [10], we should calculate the elastic energy of interaction of two vacancies (the elastic problem that has no explicit solution for the orthorhombic lattice). We propose to examine the possibility of the formation of charge order due to interaction between the charged oxygen vacancies using computer simulation by molecular dynamics method. The possibility of the formation of charge order in the classic high-temperature superconductor YBCO due to interaction between the charged oxygen vacancies or di-vacancies is examined. It was interesting to check this possibility also because the evidences were found of the connection between the charge distribution and oxygen defects in the YBCO. The discovery of oxygen "superstructures" in cuprate materials [11, 12] could help to shed light on the problem. In Ref. [11], authors observed an ordered superstructure with a periodicity of four unit cells in materials that contained oxygen vacancies, but not in samples that did not contain the oxygen defects. The formation of the superstructure depended on the oxygen concentration. In similar experiments [12], "nanodomains" of displaced copper, barium and oxygen atoms in the YBCO crystals were observed. The presence of these domains indicates that an ordered pattern of oxygen vacancies forms, leading to the same superstructure seen by [11]. As it was noted in [12], the oxygen vacancies in the Cu-O chains tend to form superstructures according to the scheme proposed by de Fontaine and co-authors [13]. In the paper [14], de Fontaine and co-authors present electronic structure calculations performed prior to the experimental observations [12] which prove that observed diffraction patterns are due to static atomic displacements around missing rows of oxygen atoms in the Cu-O plane. The phenomenon of ordering is named in [14] as O-compositional stripes.

Even though, according to [15], there is no so far unambiguous direct evidence for a static spin/charge density-wave order in the YBCO because the putative density-wave phase in the YBCO involves fluctuating rather than a static order [2], stripe-like regions were used in the atomic consideration of the structure of fluctuating density wave in the

YBCO [16]. This consideration applied recently by [16] for explanation of experimental observations [15] of electron pockets in the Fermi surface of the hole-doped YBCO. Actually, in the Fig. 1 of [16], we can see the positively charged holes situated at the oxygen di-vacancies organized in the stripe-like regions.

## II. METHOD

As the first step we analyzed the displacement field around a single charged oxygen vacancy in the bulk. We determined the spatial distribution of binding energy of charge vacancies in the di-vacancy and the displacement field around the di-vacancy. Finally we considered the conditions of the charge order formation in the vicinity of the high-angle GBs in the YBCO. It is noticed by Pennycook and co-workers [17] that first-principles calculations for realistic YBCO grain-boundary structures are computationally prohibitive. We used the molecular dynamics method in this work because it allowed us to consider consistently both bulk and defect regions of the crystal lattice. The molecular dynamics methods exploited in calculations are described in Refs. [18] and [19]. The substantial feature of the present work is the computer simulation of point defects in models of the ideal crystal lattice of the YBCO. It is worth mentioning that the computer simulation of point defects in the YBCO was done in a number of articles (see, for example, Ref. [20]), especially for calculations of the diffusion of the single oxygen vacancy in the perfect crystal lattice. In our case, we create also simultaneously two or three point defects (charged oxygen vacancies). There are four different positions of oxygen atoms in the crystal lattice of the YBCO. The vacancy was created at the position of O4 in the layer Cu1-O4 (the layer representation [21] of the YBCO lattice cell was used). The configuration of the models is as follows: the X-axis is directed along a-axis of crystal lattice, the Y-axis { along b-axis, and the Z-axis { along c-axis of the lattice, and the XOY-plane coincides with the basal ab-plane of the lattice. The creation of the charged vacancy is equivalent to the appearance of the charge  $q = 1/3 e$ , where  $e$  is the elementary charge.

In this work, we are considering also the creation of charged oxygen vacancies in the most perfect large-angle GBs { the coincident site lattice GBs with small  $\theta$  (  $\theta$  is inverse of the density of coincident sites if lattices of neighboring grains are assumed to fill all space). We will characterize the GBs by the direction of the axis of misorientation, the angle of misorientation relative to this axis, the geometrical plane of the GB which is chosen coinciding with some simple crystal lattice plane, and the repetition distance  $R_d$  along the GB. We consider the symmetric large-angle tilt GBs with the misorientation axes [001]:  $5(310)_1 = (310)_2$ , misorientation angle  $\theta = 36.87^\circ$ , repetition distance along the GB  $R_d = 3.164a$ , where  $a$  is the lattice constant along a-axis ( $a = 0.380 \text{ nm}$ );  $5(210)_1 = (210)_2$ ,  $\theta = 53.13^\circ$ ,  $R_d = 2.238a$ ;  $13(510)_1 = (510)_2$ ,  $\theta = 22.62^\circ$ ,  $R_d = 5.100a$ ;  $13(320)_1 = (320)_2$ ,  $\theta = 67.38^\circ$ ,  $R_d = 3.537a$ ;  $17(410)_1 = (410)_2$ ,  $\theta = 28.07^\circ$ ,  $R_d = 4.124a$ ;  $17(530)_1 = (530)_2$ ,  $\theta = 61.93^\circ$ ,  $R_d = 5.839a$ . Here, the boundary planes common for the two grains are given in parenthesis, and the indexes 1 and 2 refer to the two neighboring crystals of the bi-crystal. The GBs 5, 13, and 17 were chosen as the most perfect tilt GBs that cover a wide range of misorientation angles and are experimentally observable in the YBCO. In the GBs simulation, the XOZ-plane coincides with the geometrical plane of the GB. The X-axis lies in the geometrical plane of the GB. The Y-axis is perpendicular to the geometrical planes of the GB. The Z-axis is directed along the c-axis of the crystal lattice and coincides with the misorientation axis. The extent of the model along the X-axis is equal in all cases to one period of the coincident-site-lattice of the corresponding GB. The total number of ions in each model is around 600.

In Ref. [22], the interatomic potential for the YBCO was proposed. It includes pair-wise interactions consisting of the four parts: the Coulomb potential (the relative values of the charges on different atoms are determined from the requirement of producing a stable and reasonable crystal structure); the Born-Mayer-type short-range repulsive potential; the van der Waals-type potential; the Lippincott-Schroeder-type covalent potential. This interatomic potential for the YBCO has proved successfully in calculations of the minimum energy structure, the bulk modulus, the phonon spectrum, and the orthorhombic-to-tetragonal phase transition. In our study, we employ the potential [22], as well as the Ewald method of calculation. Periodic boundary conditions were applied at all the outer faces of the computational cell. The corresponding classical equations of motion were solved using the velocity form of the Verlet algorithm. Verlet algorithm is one of the most common "drift-free" higher-order algorithms [23]. The initial time step in all calculations was not greater than  $2.5 \cdot 10^{-15} \text{ s}$ . In each case of the simulation, we started with an initial configuration of the model in which all atoms, with exception of atoms removed for vacancies formation, are in their position when vacancies were absent. It took usually several thousands time steps to achieve the relaxed configuration. The comparison of the initial and final (relaxed) configurations allowed us to determine the atomic displacement vector for each atom. These displacements are shown in Fig. 1 and Fig. 2 as arrows.

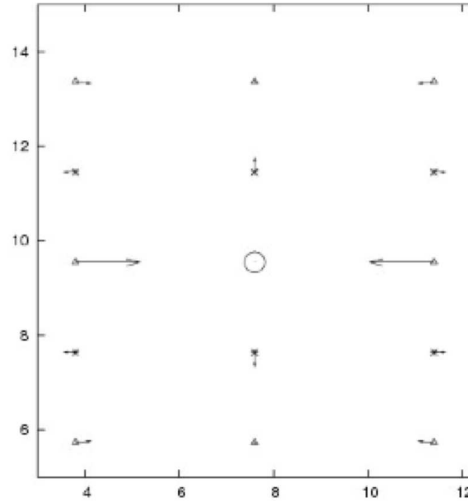


FIG. 1: Atomic displacements (shown as arrows) around a single charged vacancy O4 in the crystal lattice of the YBCO. The vacancy is situated in the basal plane that is parallel to the XOY plane of the model (the part of its top view). Only the displacements of atoms situated at the same basal plane are shown. The magnification of arrows is 4. All distances are given in angstroms. Designations of different types of atoms: Cu1  $\rightarrow$ , O4  $\circ$ .

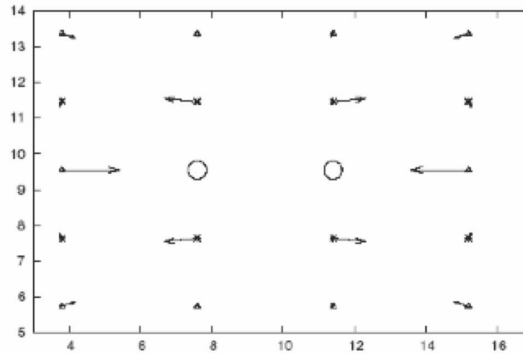


FIG. 2: Atomic displacements (shown as arrows) around a charged di-vacancy O4 in the crystal lattice of the YBCO. The di-vacancy is formed by two charged vacancies O4 lying at the basal plane. They are the first-neighbor vacancies in the direction of a-axis (X-axis in our consideration). The distance between these two vacancies is the lattice constant  $a$ . Only atoms situated at the basal plane and the components of their displacements in this plane are shown. The magnification of arrows is 2. All distances are given in angstroms. Designations of different types of atoms: Cu1  $\rightarrow$ , O4  $\circ$ .

### III. RESULTS AND DISCUSSION

The results of our calculations for the atomic displacements around a single charged vacancy O4 and a charge di-vacancy O4 in the crystal lattice of the YBCO are shown in Fig. 1 and Fig. 2. The analysis of the distribution of the atomic displacements around the single charged oxygen vacancy in ideal crystal lattice showed that this strain field is comparatively long-ranged: substantial displacements are demonstrated by atoms located at the positions of the 8th neighbors. The displacement field created by the presence of the charged oxygen vacancy is anisotropic. There are atoms that are displaced in the direction of the vacancy and there are atoms that are displaced in the opposite direction. It is clearly seen from Fig. 1: atoms O4 situated on the distances  $r = a$  from the vacancy in the basal Cu-O plane are displaced in the direction of the vacancy with the magnitude of the displacement vector  $r = 0.089a$ ; atoms Cu1 situated on the distances  $r = 0.503a$  are displaced from the vacancy with the magnitude of the displacement vector  $r = 0.020a$ . The same type of displacements are occurred for atoms outside of the basal plane: atoms O1 situated on the distances  $r = 0.693a$  from vacancy are displaced in the direction of the vacancy with the magnitude of the displacement vector  $r = 0.062a$ ; atoms Ba situated on the distances  $r = 0.767a$  are displaced from the vacancy with the magnitude of the displacement vector  $r = 0.021a$ .

Actually these results mean that some regions around the vacancy are in the state of compression, others are in the state of tension. When regions in the state of compression of one vacancy will be overlapped with regions in the state of tension of another vacancy, the total elastic energy will decrease. When like regions of two vacancies will be overlapped, the total elastic energy will increase. This should lead to the appearance of the elastic interaction between vacancies. This interaction is attractive at some mutual orientations and repulsive at others. On the atomic level, it should be revealed in a formation of stable divacancies with the positive binding energy of the vacancy in the divacancy at some mutual orientations of two vacancies in the divacancy. This assumption is supported by determination of the binding energy  $E_b^{V+V}$  of a charged oxygen vacancy in the divacancy and illustrated in the Table 1. The determination was performed as follows. According to our data, the energy of formation of the single charge oxygen vacancy O4 in the crystal lattice of YBCO equals  $E^V = 0.823 \text{ eV}$ . (The calculations of O4 vacancy formation energies in the strained and unstrained crystal lattice of YBCO by using density-functional theory in the local-density approximation yielded according to Ref. [17] correspondingly  $E^V = 1.40 \text{ eV}$  and  $E^V = 1.90 \text{ eV}$ .) The formation energy of the divacancy in the bulk from the two first-neighbor vacancies in the direction of the a-axis according to our data equals  $E^{V+V} = 1.504 \text{ eV}$ . Then the binding energy  $E_b^{V+V}$  of a charged oxygen vacancy in the divacancy equals  $E_b^{V+V} = 2E^V - E^{V+V} = 0.142 \text{ eV}$ . It is positive. Another configuration of two vacancies in the divacancy with positive binding energy is for the second-neighbor vacancies in the direction of the b-axis ( $E_b^{V+V} = 0.038 \text{ eV}$ ). Other configurations of two vacancies in the divacancy have negative binding energies.

Neighbor	$d_v$ (a,b)	$d_v$ (Å)	$E_b^{V+V}$ (eV)
1st	a	3.800	+ 0.142
2nd	b	3.820	0.699
3rd	$\sqrt{a^2 + b^2}$	5.388	0.192
4th	2a	7.600	0.295
5th	2b	7.640	+ 0.038
6th	$\sqrt{a^2 + (2b)^2}$	8.533	0.031

TABLE I: Binding energy  $E_b^{V+V}$  of the charged O4 vacancy in the divacancy depending on a distance  $d_v$  between vacancies in Cu1-O4 plane of the high-temperature superconductor  $\text{YBa}_2\text{Cu}_3\text{O}_7$ .

$R_d$ (a)	2.238	3.164	3.537	4.124	5.100	5.839
GB	5	5	13	17	13	17
	53.13	36.87	67.38	28.07	22.62	61.93
$E_b^{GB+em b}$ (eV)	6.51	10.13	38.06	34.08	51.13	107.77

TABLE II: Adsorption capability of grain boundaries in the  $\text{YBa}_2\text{Cu}_3\text{O}_7$  with respect to the stripe embryo formation.

The distribution of displacements around the divacancy is shown in Fig. 2. Divacancy is formed by two charged vacancies O4 situated at the distance of one lattice constant  $a$  from each other in the basal plane. In Fig. 2, only the displacements of atoms lying in the same basal plane are shown. Therefore, there is a good possibility to compare the displacement fields around the single vacancy and divacancy. It should be pointed out that the magnification of the displacements in Fig. 1 is 4, but in Fig. 2 it is only 2. There are following displacements around the divacancy: atom O4 is displaced in the direction of the divacancy with the magnitude of the displacement vector  $r = 0.212a$ , which is 2.390 times greater than for a single vacancy; atom Cu1 is displaced from the divacancy with the magnitude of the displacement vector  $r = 0.105a$ , which is more than 5 times greater than for a single vacancy. Therefore, based on these results and by analogy with displacement field of the single vacancy, one can expect that anisotropy of the displacement field around divacancies should lead to the appearance of interaction between them: the attraction at some mutual orientations and repulsion at others. Some specific positions of the divacancies should result in decrease of the elastic energy and lead to a formation of stable configurations of the divacancies with the positive binding energy of the vacancies in such configurations. The consideration [8, 9] showed, that if the interaction of the impurities in crystals is long-range and intrinsically anisotropic (attractive in certain directions and repulsive in others), then the charge order may appear. It was shown above that interaction between charged oxygen vacancies and divacancies in the YBCO is long-range and intrinsically anisotropic (attractive in certain directions and repulsive in others). Thus, we can expect that there is, in principle, the possibility of the charge order formation in the YBCO by vacancies or by divacancies. But actually important question is what should be the trend when more charge vacancies will be

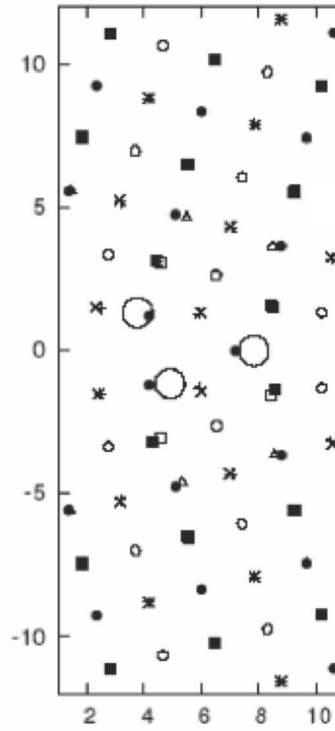


FIG. 3: Projection of the positions of atoms at the grain boundary  $\Gamma_7$ ,  $\theta = 28.07^\circ$  with the stripe embryo inside (consisted of three vacancies) on the plane XOY (this plane coincides with the basal plane of the YBCO crystal lattice). All distances are given in angstroms. Designations of different types of atoms: Y —  $\circ$ , Ba —  $\blacksquare$ , Cu1 —  $*$ , Cu2 —  $\square$ , O1 —  $\circ$ , O2 —  $\bullet$ , O3 —  $\triangle$ , O4 —  $\bullet$ .

considered? To get the answer on this question, we examined the energy formation of the small chain of three charged first neighbor oxygen vacancies along the a-axis.

The formation energy of the small chain of three charged first neighbor oxygen vacancies along the a-axis according to our data equals  $E^{V+V+V} = 2.939 \text{ eV}$ . Therefore, the formation energy of additional third vacancy equals  $1.435 \text{ eV}$ . It is greater than  $E^V$ . As a result, the binding energy of the vacancy in this configuration is negative and equals  $0.470 \text{ eV}$ . Thus, there is the energy disadvantage of the formation of charge order by comparatively long chains of charged vacancies. Therefore, we can expect that the charge order formation by charged oxygen vacancies first of all will be formed near the crystal lattice defects. Most relevant defects are the GBs. We can expect the excess of oxygen vacancies both in the low-angle and high-angle GBs (see, for example, [17, 19]).

It was found in [24] that the in-plane resistivity anisotropy in single crystals of YBCO gives evidence for conducting charge stripes. The data indicate that intrinsically conducting stripes govern the transport in samples with  $T_c$  of as high as  $50 \text{ K}$ . It is well known that GBs play extremely important role in transport properties of the YBCO polycrystals (see, for example, the review [25]). Therefore, it is important to understand relationship between charge stripes formation, their transport properties and the GBs in the YBCO. It is logical to suggest that transparency or non-transparency of GBs with the respect to the stripes depends on the energy advantage or disadvantage of stripe embryo formation in the GBs.

We consider as a model of the stripe embryo configuration of three charged oxygen vacancies in which one vacancy is located directly in the GB plane, two other vacancies are at first neighbors positions of O4 atoms. They are situated from both sides of the GB plane and each vacancy in its own grain as shown in Fig. 3. Generally speaking, we can imagine other configurations of the stripe embryo, for example, the stripe embryo as a linear-type configuration of the vacancies piercing the GB. But, in the case of the linear-type configuration, the stripes in the neighboring grains should start from different points of the GB. So, we can expect smaller their influence on the transport properties of the GB. The projection of the positions of atoms at the GB  $\Gamma_7$ ,  $\theta = 28.07^\circ$  with the stripe embryo inside on the plane XOY is shown in Fig. 3.

To determine the adsorption capability of the large-angle GBs with respect to the embryo of stripes formation we expanded approach [19], where the computer simulation of single vacancies in the YBCO was done. The adsorption capability of the GB can be characterized by  $E_b^{GB+emb}$  — the binding energy of the stripe embryo with the GB.

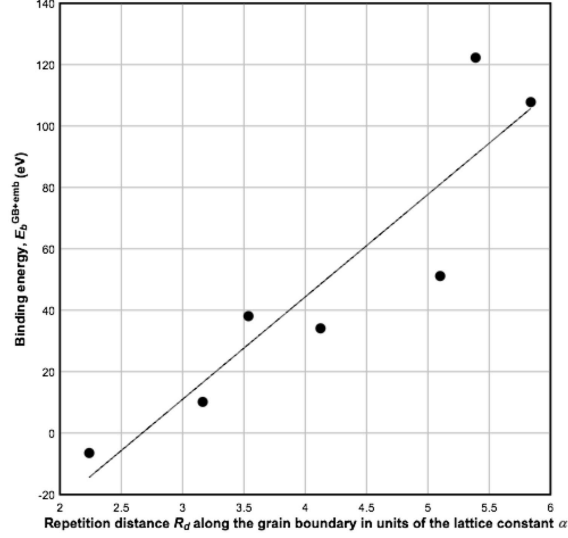


FIG. 4: Binding energy stripe embryo with grain boundary versus repetition distance along grain boundary.

$E_b^{GB+emb}$  can be estimated as follows:

$$E_b^{GB+emb} = E^{GB} - E^{GB+emb}; \quad (1)$$

where  $E^{GB}$  is the energy of the microcrystallite containing the perfect grain boundary and  $E^{GB+emb}$  is the energy of the microcrystallite containing grain boundary with the stripe embryo. The results of the computer simulation are presented in Table 2. A analysis of the computer simulation data for the different GBs shows, that GB 5, = 53:13 with the smallest repetition distance has negative  $E_b^{GB+emb}$ . All other analyzed GBs have positive  $E_b^{GB+emb}$ . It means that there is an energy advantage of the embryo stripe formation in all of these GBs. There is some correlation between  $E_b^{GB+emb}$  and  $R_d$ , but much more distinct dependence close to linear is found between  $E_b^{GB+emb}$  and the repetition distance  $R_d$  of the GB as shown in Fig. 4. This dependence can be approximated by the best-fit linear regression line  $y = 33.366x - 89.112$ , with the coefficient of determination  $R^2 = 0.833$ . Thus, there is a linear correlation between  $E_b^{GB+emb}$  and repetition distance  $R_d$ . We think that this linear regression approximation can be used to estimate the  $E_b^{GB+emb}$  not only for GBs analyzed in this article but for different GBs observed in physical experiments.

It was shown above that there is energy disadvantage of the formation of charge order by comparatively long chains of charged vacancies in the bulk. At the same time, the stripe embryo formation at all high-angle GBs (with the exclusion only GB 5, = 53:13) leads to decrease of energy and allows additional vacancies to get into formation with the stripe embryo. One can expect that a type of GB may determine the character of the initiated charge order inside of a grain, and that GBs may play a special role in the adjustment of charge orders in neighboring grains. This assumption, of course, should be strictly examined. The presence of stripes may substantially influence the transport properties of GBs in high- $T_c$  superconductors. It is difficult now to estimate this influence, but if the experimental studies of the charge order in the high- $T_c$  superconductors usually were performed in the single crystals, one can expect that corresponding experiments performed on the bi-crystals containing high-angle GBs also to be of interest to charge order formation and its influence on the transport properties of GBs in the YBCO.

#### IV. CONCLUSION

Thus, based on approach [8, 9] and our results, one can conclude that there is a possibility of the charge order formation consisted of the charged oxygen vacancies or divacancies in the YBCO. The high-angle GBs regions are preferable places for the charge order formation in the YBCO. It should be interesting to verify experimentally on the bi-crystals containing the high-angle GBs the charge order formation and its influence on the transport properties of the GBs in the YBCO. It can be expected that obtained above results might be qualitatively applied to the other cuprate high-temperature superconductors because they consist of the parallel Cu-O planes, similar to such in the YBCO, with other elements sandwiched in between these planes.

Acknowledgment: The authors express thanks to A.B. Kuklov for a useful discussion. This work is supported by grant from the City University of New York PSC-CUNY Research Award Program (Project Number: 68061-0037).

- 
- [1] J.A. Robertson, S.A. Kivelson, E. Fradkin, A.C. Fung, and A. Kapitulnik, *Phys. Rev. B* 74, 134507 (2006).
  - [2] S. Kivelson, I. Bindloss, E. Fradkin, V. Oganesyan, J. Tranquada, A. Kapitulnik, and C. Howald, *Rev. Mod. Phys.* 75, 1201 (2003).
  - [3] J. Zaanen, *Nature* 440, 1118 (2006).
  - [4] J. Zaanen and O. Gunnarson, *Phys. Rev. B* 40, 7391 (1989).
  - [5] K. Machida, *Physica C* 158, 192 (1989).
  - [6] V. Emery, S. Kivelson, and H. Lin, *Phys. Rev. Lett.* 64, 475 (1990).
  - [7] J. Tranquada, B. Sternlieb, J. Axe, Y. Nakamura, and S. Uchida, *Nature* 375, 561 (1995).
  - [8] D. Khomskii and K. Kugel, *Europhys. Lett.* 55, 208 (2001).
  - [9] D. Khomskii and K. Kugel, *Phys. Rev. B* 67, 134401 (2003).
  - [10] J.D. Eshelby, in *Solid State Physics*, edited by F. Seitz and D. Turnbull, vol. 3 of *Advances in research and applications of solid state physics*, pp. 79-190, Academic Press, New York (1956).
  - [11] J. Strempfer, I. Zegkinoglou, U. Rutt, M. Zimmermann, C. Bernhard, C. Lin, T. Wolf, and B. Keimer, *Phys. Rev. Lett.* 93, 157007 (2004).
  - [12] Z. Islam, X. Liu, S. Sinha, J. Lang, Moss, D. Haskel, G. Srajer, P. Wochner, D. Lee, D. Haefer, and U. Welp, *Phys. Rev. Lett.* 93, 157008 (2004).
  - [13] G. Ceder, M. Asta, W. Carter, M. Kraichnan, D. de Fontaine, M. Mann, and M. Sluiter, *Phys. Rev. B* 41, 8698 (1990).
  - [14] D. de Fontaine, V. Ozols, Z. Islam, and S. Moss, *Phys. Rev. B* 71, 212504 (2005).
  - [15] D. LeBoef, N. Doiron-Leyraud, J. Levallois, R. Daou, J.B. Bonnemaison, N.E. Hussey, L. Balicas, B.J. Ramshaw, R. Liang, D.A. Bonn, W.N. Hardy, S. Adachi, C. Proust, and L. Taillefer, *Nature* 450, 533 (2007).
  - [16] C. P. Eiderer and R. Hackl, *Nature* 450, 492 (2007).
  - [17] R.F. Klie, J.P. Buban, M. Varela, A. Franceschetti, C. Jooss, Y. Zhu, N.D. Browning, S.T. Pantelides, and S.J. Pennycook, *Nature* 435, 475 (2005).
  - [18] V.S. Boyko and A.M. Levine, *Phys. Rev. B* 64, 224525 (2001).
  - [19] V.S. Boyko, R. Ya. Kezerashvili, and A.M. Levine, *Phys. Rev. B* 69, 212502 (2004).
  - [20] X. Zhang and C.R.A. Catlow, *Molecular Simulation* 12, 115 (1994).
  - [21] C.P. Poole, H.A. Farach, and R.J. Creswick, *Superconductivity*, Academic Press, San Diego, New York (1995).
  - [22] S.L. Chaplot, *Phys. Rev. B* 42, 2149 (1990).
  - [23] H. Gould and J. Tobochnik, *An introduction to computer simulation methods: applications to physical systems*, vol. 1, Addison-Wesley Publishing Company, Reading, MA - Menlo Park, CA - New York (1988).
  - [24] Y. Ando, K. Segawa, S. Komiyama, and A. Lavrov, *Phys. Rev. Lett.* 88, 137005 (2002).
  - [25] H. Hlgencamp and J. Mannhart, *Rev. Mod. Phys.* 74, 485 (2002).